Using a squeegee on a layer of viscous or viscoplastic fluid

John R. Lister *
Department of Applied Mathematics and Theoretical Physics, University of Cambridge, Cambridge CB3 0WA, United Kingdom

Edward M. Hinton
School of Mathematics and Statistics, The University of Melbourne, Parkville, VIC 3010, Australia

(Received 12 March 2022; accepted 20 September 2022; published 13 October 2022)

We use lubrication theory to study the bow wave ahead of a squeegee as it moves steadily over a horizontal layer of fluid. If the squeegee is infinitely long with a small gap at its base then the motion is two dimensional and we obtain an analytic prediction for the flow thickness. For a relatively long straight squeegee on a layer of viscous fluid with no gap, we deploy a two-dimensional approximation, which enables the flow thickness in the bow wave to be determined relative to the thickness at the squeegee. The analysis is completed by balancing the flux into the bow wave with the transverse flux perpendicular to the squeegee associated with hydrostatic pressure gradients. The simple method is adapted to squeegees that are angled to the direction of translation. For a layer of viscoplastic fluid that has a relatively high yield stress, the bow wave is quasiplugged and this observation enables a different flux balance to be used to determine the flow thickness. The predictions are compared favorably to numerical results.

DOI: 10.1103/PhysRevFluids.7.104101

I. INTRODUCTION

Flows that are driven predominantly by gravity and resisted by viscous stresses, known as "viscous gravity currents," occur in many industrial and environmental settings. Often these flows interact with obstructions. Examples include the deflection of lava flows by barriers [1] and the manufacture of electronic components through screen printing in which a blade or squeegee is used to evenly distribute material over a surface [2–4].

In this paper, we study the steady inertialess interaction between a moving squeegee and a thin layer of viscous fluid. Provided the squeegee is relatively long, the flow is quasi-two-dimensional enabling the flow thickness in the bow wave to be determined up to a slowly varying function of the lateral position. Simple flux-balance arguments are deployed to obtain this function. The ideas are relevant to the interesting problem of screen printing. In addition, they provide insight and a novel pedagogical approach to understanding the interaction of inertialess flows with obstructions. Indeed, our uncomplicated analysis is straightforwardly adapted to squeegees of arbitrary shape and to the case of a layer of viscoplastic fluid.

The theory can be extended to a wide range of applications in other areas of continuum mechanics. These include flows in porous media, settings in which surface tension plays a dominant role, and flows down slopes; see, e.g., Ref. [5]. Another possible extension is to the transient flow that arises when a squeegee bulldozes a mound of fluid, which has been investigated for granular material [6].

*lister@damtp.cam.ac.uk

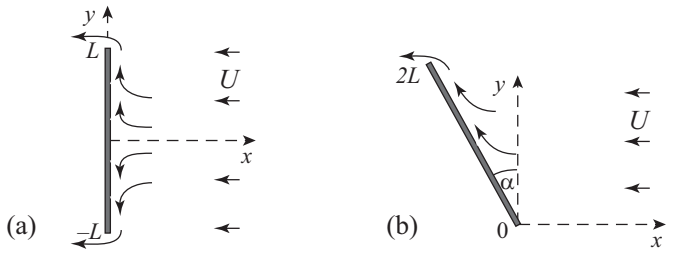

FIG. 1. (a) In the reference frame of a squeegee of length $2L$, a plane covered with viscous fluid moves from right to left with speed U. Fluid builds up in a bow wave ahead of the squeegee and is diverted laterally around the ends by the pressure gradient in the y direction. (b) The squeegee is now inclined at angle α to the y axis and flow in the bow wave to the trailing end of the squeegee is primarily due to the component $U\sin\alpha$ of the plane's velocity parallel to the squeegee.

The paper is structured as follows. In Sec. II, the technique is presented for the case of straight and angled squeegees and a layer of Newtonian viscous fluid. We use a shallow approximation. We allow slip at the squeegee boundary (as is required for lubrication theory) and neglect Moffat eddies in the corner, but note that these features could be reintroduced with additional effort [7,8]. In Sec. III, we show that the same ideas, applied with some key differences, furnish the flow thickness in the squeegee bow wave for a general viscoplastic fluid with a relatively high yield stress. The theory is compared to some numerical computations. Applications of such non-Newtonian rheologies might include the bulldozing of mud or slurry, or the scraping of sediments from subducting oceanic lithosphere to form a deep accretionary wedge [9,10]. We conclude in Sec. IV.

II. NEWTONIAN FLUID

In this section, we describe the problem of squeegeeing a layer of viscous fluid on a horizontal plane or of using a snowplow to clear up a large pool of molasses [11]. The emphasis here is on showing how simple flux arguments can be used to determine the structure of the bow wave.

Consider a horizontal plane $z = 0$ covered with a thin layer of viscous fluid of uniform initial thickness h_∞. We model the squeegee (window-wiper blade or scraper) as a thin vertical rigid planar barrier of some horizontal extent $2L \gg h_\infty$ in the y direction and of large vertical extent (Fig. 1). The squeegee is moved slowly and horizontally at a constant speed U perpendicular to its plane, sweeping up the fluid ahead of it.

For convenience, we work in the reference frame of the squeegee so that the plane moves with speed $-U$. Neglecting surface tension and assuming lubrication theory, the evolution of the film thickness $h(x, y, t)$ due to gravitational flattening is given by

$$\frac{\partial h}{\partial t} - U\frac{\partial h}{\partial x} = \frac{\rho g}{3\mu}\nabla\cdot(h^3\nabla h), \tag{1}$$

where $\nabla = (\partial/\partial x, \partial/\partial y)$. By balancing the second and third terms, we see that the natural horizontal length scale for the bow wave ahead of the squeegee is $\ell = \rho g h_\infty^3/\mu U$. The usual conditions $h_\infty \ll \ell$ and $\rho U h_\infty^2/\mu\ell \ll 1$ for lubrication theory to hold reduce to $U \ll \rho g h_\infty^2/\mu$ and $U^2 \ll g h_\infty$, respectively. Within an $O(h)$ distance of the squeegee the lubrication description breaks down and the local flow resembles the classic corner-flow (or "paint scraper") problem; see, e.g., Ref. [12], p. 224 ff. Here, however, we are concerned with the flow on the larger $O(\ell)$ length scales.

We make the problem dimensionless by scaling h by h_∞, all horizontal lengths by ℓ, and time by ℓ/U. The dimensionless equations are then

$$\frac{\partial h}{\partial t} - \frac{\partial h}{\partial x} = \frac{1}{3}\nabla\cdot(h^3\nabla h), \tag{2}$$

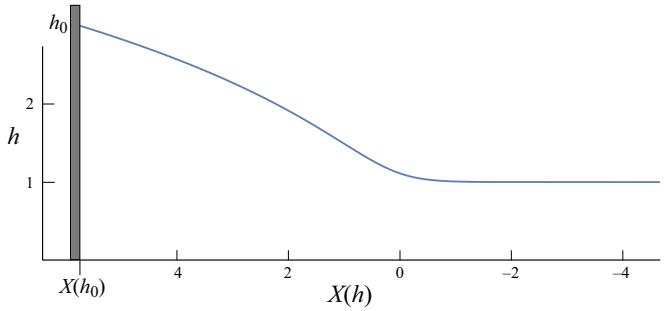

FIG. 2. Dimensionless profile (4) of the bow wave ahead of the squeegee. The profile extends further to the left if the height h_0 at the squeegee is greater. The dimensional scales for h and X are h_∞ and $\ell = \rho g h_\infty^3/\mu U$ and it is assumed that $h_\infty/\ell \ll 1$ so that lubrication theory is valid except very close to the squeegee.

where $h \to 1$ as $x \to \infty$, the squeegee is at $x = 0$ for $-\mathcal{L} \leqslant y \leqslant \mathcal{L}$, and the dimensionless squeegee half length is $\mathcal{L} = \mu U L/\rho g h_\infty^3$.

A. Infinitely long squeegee

It is instructive first to consider the limit $\mathcal{L} \to \infty$ of an infinitely long squeegee with a small gap of height $\epsilon \ll 1$ beneath it. The small gap allows for a steady state $h(x)$ to be established in which a sufficiently large bow wave has built up ahead of the squeegee that the hydrostatic pressure forces a unit leakage flux through the gap to balance that arriving from $x = \infty$. The equation for this steady state,

$$-\frac{dh}{dx} = \frac{1}{3}\frac{d}{dx}\Big(h^3\frac{dh}{dx}\Big), \tag{3}$$

can readily be integrated to obtain first $3(1-h) = h^3(dh/dx)$ and then the implicit equation

$$x = X(h_0) - X(h), \quad \text{where } X(h) \equiv \frac{1}{3}\int \frac{h^3 dh}{h-1} = \frac{1}{3}\big\{\tfrac{1}{3}h^3 + \tfrac{1}{2}h^2 + h + \ln(h-1)\big\}, \tag{4}$$

see Fig. 2, where h_0 is whatever height is needed at $x = 0$ to drive the leakage flux. For a rectangular gap of height and width $O(\epsilon)$, scaling shows that h_0 is $O(\epsilon^{-1})$; for a gap of minimum height ϵ formed by a semicircular lower boundary of radius $\delta \gg \epsilon$, a standard lubrication-theory calculation shows that h_0 is $O(\delta^{1/2}/\epsilon^{5/2})$. The main point is that h_0 needs to be $\gg 1$ if $\epsilon \ll 1$. The shape (4) of this bow wave is analogous to the flat pond in Hinton *et al.* [5], Eq. (45).

The evolution of $h(x,t)$ to the steady state can be evaluated by a simple flux argument: we assume, to be verified, that the accumulating bow wave has a quasisteady shape given by (4) with h_0 replaced by $h(0,t)$. Under this assumption, the area of excess fluid accumulated ahead of the squeegee is

$$A(t) = \int_0^\infty (h-1)\,dx = \int_1^{h(0,t)} (h-1)\frac{dX}{dh}dh = \frac{1}{12}\big\{h(0,t)^4 - 1\big\}. \tag{5}$$

The leakage flux q_L under the squeegee is proportional to the hydrostatic pressure h at leading order and is equal to unity when $h = h_0$ in steady state. Hence $q_L = h(0,t)/h_0$. Unit flux is arriving from $x = \infty$ by advection and thus $dA/dt = 1 - h(0,t)/h_0$ by mass conservation. Substituting from (5), we obtain an implicit equation,

$$t = \frac{1}{3}\int_1^{h(0,t)} \frac{h^3\,dh}{1 - h/h_0}, \tag{6}$$

for $h(0,t)$. We note that, for $1 \ll h(0,t) \ll h_0$, Eqs. (6) and (4) give $h(0,t) \sim (12t)^{1/4}$ and $X(h(0,t)) \sim (192t)^{3/4}$, from which it can be verified by scaling that the assumption of a quasisteady shape is justified. Conservation of mass shows that the film thickness left behind the squeegee is given by $q_L(t)$, which increases slowly to 1 as the bow wave builds up to steady state.

B. Long finite squeegee

We now return to the original problem of a long but finite squeegee, $1 \ll \mathcal{L} < \infty$, with no gap beneath it ($\epsilon = 0$). For a steady state $h(x,y)$ to be established ahead of the squeegee, the flux arriving at the squeegee from $x = \infty$ must be diverted sideways around the ends at $y = \pm\mathcal{L}$.

The solution can again be obtained by a simple flux argument and an appropriate approximation for the shape of the bow wave. There is no flux through the squeegee and no flux across $y = 0$ by symmetry. In steady state the flux from $x = \infty$ in $0 < y < Y$ due to the translation must therefore be equal to the flux across $y = Y$ due to the lateral pressure gradient $\partial h/\partial y$. Thus

$$y = \int_0^\infty -\tfrac{1}{3}h^3(\partial h/\partial y)\,dx = -\frac{1}{12}\frac{d}{dy}\int_0^\infty (h^4 - 1)\,dx. \tag{7}$$

We now assume, to be verified, that the shape of the bow wave is given by (4) with the height at the squeegee $h_0(y)$ varying slowly along the length of the squeegee in such a way that (7) is satisfied. We also assume that the diverted flux goes around the ends of the squeegee close to $y = \pm\mathcal{L}$ so that, at leading order, $h_0(\pm\mathcal{L})$ is very much smaller than the interior values. Equation (7) can be integrated with respect to y and the x integral evaluated exactly using $dx = (dX/dh)dh$ to find

$$6(\mathcal{L}^2 - y^2) = \tfrac{1}{21}h_0^7 + O\big(h_0^6\big). \tag{8}$$

To leading order for $\mathcal{L} \gg 1$, we deduce that

$$h_0(y) \sim \{126(\mathcal{L}^2 - y^2)\}^{1/7}, \tag{9}$$

except near $y = \pm\mathcal{L}$, and the assumed shape of the bow wave is then given by (4) and (9). This theoretical prediction compares very well with a numerical solution to the full problem in Figs. 3(a) and 3(b).

The assumption that the shape of the bow wave is given by (4) at leading order is valid if $h(x,y)$ varies more rapidly in the x direction than the y direction. Since for $\mathcal{L} \gg 1$ we have $X(h_0) \sim \frac{1}{9}\{126(\mathcal{L}^2 - y^2)\}^{3/7} = O(\mathcal{L}^{6/7})$ and $\mathcal{L}^{6/7} \ll \mathcal{L}$, this assumption is asymptotically valid along most of the squeegee. However, it fails sufficiently close to the ends, at $\mathcal{L} \mp y = O(\mathcal{L}^{3/4})$, where flow predominantly parallel to the squeegee gives way to a fully two-dimensional flow around the end.

C. Snowplow problem

Finally, we consider the snowplow problem or, equivalently, a squeegee whose blade is held at an angle α ($0 < \alpha < \pi/2$) to the y axis [see Fig. 1(b)]. For convenience, we take the origin to be at the leading end of the squeegee so that the trailing end is at $(-2\mathcal{L}\sin\alpha, 2\mathcal{L}\cos\alpha)$. As should be intuitively obvious from experience, the tilting of the squeegee makes it easier to push the fluid to one side and reduces the magnitude of the bow wave.

Once again, a simple flux argument and approximation of the bow-wave profile yields the answer. The unit flux arriving from $x = \infty$ at the squeegee must be diverted to run along the squeegee until it reaches the trailing end. With the leading end at the origin, the total flux diverted along the squeegee at position y in the bow wave is simply $Q(y) = y$ ($0 < y < 2\mathcal{L}\cos\alpha$).

To analyze the structure of the bow wave, we resolve the velocity of the plane into components $\sin\alpha$ parallel to the squeegee and $\cos\alpha$ perpendicular to the squeegee. We assume, to be verified, that the height of the bow wave varies more rapidly in the direction perpendicular to the squeegee

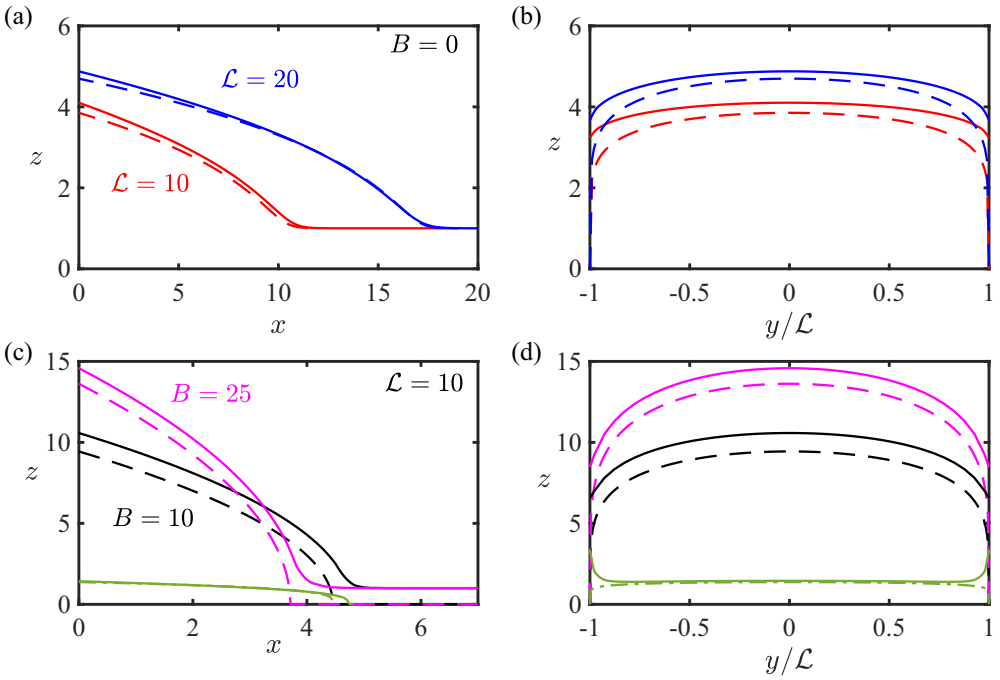

FIG. 3. Comparison between the numerical results (solid lines) and the leading-order theoretical predictions (dashed lines) for the dimensionless flow thickness with a straight squeegee. (a),(b) Along the center line ($y = 0$) and at the squeegee ($x = 0$) for a Newtonian fluid with $\mathcal{L} = 10, 20$ [Eqs. (4) and (9)]. (c),(d) Along the center line and at the squeegee for a Bingham fluid with $B = 10, 25$ and $\mathcal{L} = 10$ [Eqs. (17) and (22)]. The green lines show the numerical and theoretical predictions for the yield surface for $B = 10$. In all cases the dimensional vertical and horizontal scales differ by a factor $h_\infty/\ell \ll 1$.

than in the parallel direction. Its shape is thus given by

$$-\cos\alpha\,\frac{\partial h}{\partial x'} = \frac{1}{3}\,\frac{\partial}{\partial x'}\Big(h^3\,\frac{\partial h}{\partial x'}\Big), \tag{10}$$

where x' is a coordinate perpendicular to the squeegee and the factor $\cos\alpha$ is the perpendicular component of the plane's velocity. The solution is $x'\cos\alpha = X(h_0) - X(h)$, where $h_0(y)$ varies slowly along the squeegee. The extra flux parallel to the squeegee in the bow wave is dominated by the parallel component of advection with speed $\sin\alpha$ and is thus equal to

$$\sin\alpha\int_0^\infty (h-1)\,dx' = \tfrac{1}{12}\tan\alpha\big(h_0^4 - 1\big). \tag{11}$$

Equating this to the diverted flux $Q(y)$, we find that the height of the bow wave at the squeegee is given by

$$h_0(y) = \{1 + 12\,\cot\alpha\,y\}^{1/4} \tag{12}$$

for $0 < y < 2\mathcal{L}\cos\alpha$. As anticipated, tilting reduces the magnitude and width of the bow wave, from $O(\mathcal{L}^{2/7})$ to $O(\mathcal{L}^{1/4})$ and from $O(\mathcal{L}^{6/7})$ to $O(\mathcal{L}^{3/4})$, respectively. Since $\mathcal{L}^{3/4} \ll \mathcal{L}$, the assumed shape of the bow wave is asymptotically valid along most of the squeegee. Sufficiently close to the trailing end, $2\mathcal{L}\cos\alpha - y = O(\mathcal{L}^{3/4})$, the approximations fail and there is again a fully two-dimensional flow around the end [see Fig. 4(a)]. Close to the leading end, where $h_0 = O(1)$, the flow is also fully two dimensional.

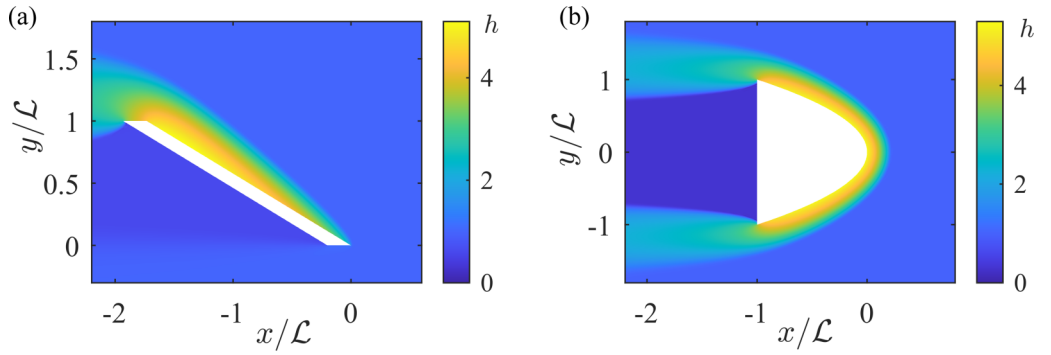

FIG. 4. Steady flow thickness from numerical solutions of (2) for Newtonian flow around (a) a squeegee at angle $\alpha = \pi/3$ and (b) a parabolic squeegee. In both cases $\mathcal{L} = 100$. Except near the ends, the solution is described asymptotically by the theory in Sec. II C.

Equation (12) also holds for a curved squeegee if the local angle $\alpha(y)$ between the squeegee and the y axis satisfies $0 < \alpha(y) < \pi/2$; separate analysis would be needed for the singular cases $\alpha = 0$ ($\cot\alpha = \infty$) and $\alpha = \pi/2$ ($\cos\alpha = 0$) which occur, for example, at the front and sides of a semicircular shape. As another example, since $\cot\alpha = dy/dx$, Eq. (12) predicts a constant height bow wave for a parabolic squeegee [see Fig. 4(b)], which is thus optimal for avoiding overtopping.

Another variation asks when leakage beneath a finite squeegee is significant compared to the flux diverted sideways. There is also an interesting question of how the ridge of fluid diverted around the ends of the squeegee starts to spread to fill the gap left behind the squeegee. (See [13] for the downslope case.)

III. BINGHAM FLUID

In this section, we consider squeegeeing a layer of viscoplastic fluid. We illustrate the analysis with a Bingham fluid, which is the simplest constitutive model for such a fluid: for stresses below a certain yield stress τ_Y, the material behaves rigidly; for stresses larger than τ_Y, the material flows with constant viscosity μ in response to the excess stress. We present flux-balance arguments to describe the bow wave in the case that the material has a relatively large yield stress. While the main assumption of the analysis, that gradients in thickness are much larger perpendicular to than parallel to the squeegee, is the same as in the Newtonian case, the yield-stress condition requires a different method of solution.

For gravity-driven flow in a thin layer, the pressure is hydrostatic and the dimensional shear stress, $\rho g(h-z)\nabla h$, varies linearly from zero at the free surface ($z = h$) to a maximum at the base ($z = 0$) [14,15]. Hence, if the shear stress at $z = 0$ is less than the yield stress τ_Y, then the entire layer is rigid and static. Conversely, if the stress at $z = 0$ exceeds the yield stress, then there is a positive height

$$Z(x, y, t) = h - \frac{\tau_Y}{\rho g|\nabla h|}, \tag{13}$$

where the shear stress equals the yield stress, and this height divides the flow into two regions: in the lower region $0 < z < Z$ the material is clearly yielded and flows viscously with a parabolic velocity profile whose gradient vanishes at the (apparent) yield surface $z = Z$; in the upper region $Z < z < h$ the material moves (apparently) rigidly in plug flow. (Detailed asymptotic analysis of thin-layer flow [14] shows that the upper region is actually weakly yielded due to horizontal variations in velocity and the attendant stresses; the upper region is termed a "pseudoplug" and $z = Z$ a "fake" yield surface. These higher-order subtleties do not affect the leading-order analysis below.) The evolution

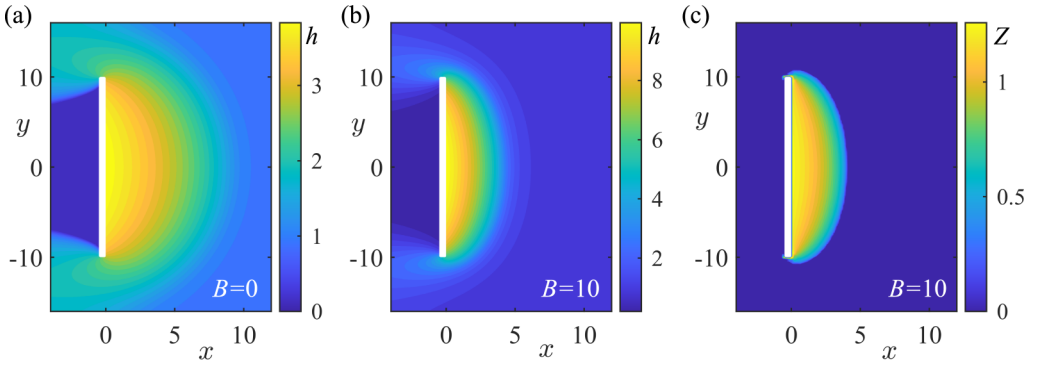

FIG. 5. Steady flow thickness around a straight squeegee of half length $\mathcal{L} = 10$ calculated numerically. (a) Newtonian fluid, $B = 0$. (b) Bingham fluid with $B = 10$. (c) The height of the yield surface for $B = 10$. Note the different color scales in each panel.

equation for the film thickness $h(x, y, t)$ is obtained by vertical integration of the velocity profile across both regions followed by use of mass conservation as usual [15].

We retain the moving coordinate system of Sec. II. We scale thicknesses with h_∞, horizontal lengths by $\ell = \rho g h_\infty^3/(\mu U)$, and time by ℓ/U, as in the Newtonian case, in order to obtain the dimensionless evolution equation

$$\frac{\partial h}{\partial t} - \frac{\partial h}{\partial x} = \frac{1}{3}\nabla \cdot \left[\frac{1}{2}Z^2(3h - Z)\nabla h\right], \tag{14}$$

where

$$Z = \max\left\{h - \frac{B}{|\nabla h|}, 0\right\}, \quad B = \frac{\tau_Y h_\infty}{\mu U}. \tag{15}$$

The Bingham number B represents the magnitude of the yield stress relative to viscous stresses and the evolution equation (14) reduces to the Newtonian case (2) when $B = 0$ and $Z = h$. The boundary conditions are $h \to 1$ as $x \to \infty$ and no flux into the squeegee at $x = 0$, $-\mathcal{L} \leqslant y \leqslant \mathcal{L}$, where $\mathcal{L} = \mu U L/(\rho g h_\infty^3) = L/\ell$, as in the Newtonian case.

The steady version of (14) was solved numerically using the finite-element package of MATLAB's Partial Differential Equation toolbox. A rectangular domain was used with boundary condition $h = 1$ on the right-hand edge and $\partial h/\partial n = 0$ on the other three edges. At the squeegee, a no-flux boundary condition was applied. The Bingham constitutive law was regularized following the Appendix in [15].

Results for the flow thickness for a straight squeegee of half length $\mathcal{L} = 10$ are shown in Fig. 5(a) for a Newtonian fluid and in Fig. 5(b) for a Bingham fluid with $B = 10$. Note the different thickness scales in the panels. The Bingham fluid accumulates in a much deeper, but more localized, bow wave. Figure 5(c) shows the height of the yield surface corresponding to Fig. 5(b). The bow wave is defined by the finite region where $Z > 0$, and outside this region $Z = 0$. Figure 5 also demonstrates that $Z \ll h$ so that the fluid is in plug flow over most of its thickness, even in the bow wave. These observations are borne out by the theory in the following subsections.

A. Infinitely long squeegee

We begin the analysis of a Bingham fluid by considering the steady flow upstream of an infinitely long squeegee with a small gap underneath it. A large bow wave builds upstream of the squeegee.

The equation for the steady state is

$$1 = h + \frac{1}{6}Z^2(3h - Z)\frac{dh}{dx}, \quad \text{where } Z = \max\left\{h + \frac{B}{dh/dx}, 0\right\}, \tag{16}$$

since $dh/dx < 0$. This is a nonlinear first-order ordinary differential equation for $h(x)$, which can be integrated numerically for given B. In contrast to the Newtonian case, the bow wave of Bingham fluid has finite extent and there is a qualitative change in behavior at its edge [e.g., Fig. 5(c)]. Within the bow wave, the fluid is yielded in a thin layer $0 < z < Z$ and $h > 1$; upstream of the bow wave, the fluid is completely unyielded $Z = 0$ and $h = 1$.

In the regime $B \gg 1$ of a large yield stress, we anticipate that the flow in the bow wave is plugged over most of its thickness, which corresponds to $0 < Z \ll h$. Under this assumption, Eq. (16 b) becomes $0 = h + \frac{B}{dh/dx}$ at leading order, which furnishes the solution

$$h(x) = \left[h_0^2 - 2Bx\right]^{1/2}. \tag{17}$$

The height h_0 at the squeegee is whatever is needed to drive unit leakage flux through the small gap and the bow wave (17) has a finite extent $X(h_0) = (h_0^2 - 1)/2B$. If $Z \ll h$, Eq. (16) also provides the approximation

$$Z^2 = 2(h - 1)/B, \tag{18}$$

which confirms the consistency of the assumption that $Z \ll h$ for $B \gg 1$. The corrections to Eqs. (17) and (18) are $O(Z/h)$ in relative magnitude. [We note in passing that the sudden transition from $Z = 0$ in $x > X$ to $Z > 0$ in $x < X$ suggests there is a local nonuniformity in the thin-layer asymptotic analysis of [14], which might be resolved over a short transition region of dimensional width $O(h_\infty)$. This small region would have no effect on the large scale flow.]

B. Long finite squeegee

In this section, we consider a long finite squeegee with no gap beneath it and a fluid with relatively large yield stress ($B \gg 1$) so that the steady flow in the bow wave is again quasiplugged (i.e., plugged over most of its thickness). As in Sec. II B, we assume (condition to be determined *a posteriori*) that the thickness of the bow wave varies more rapidly in the x direction than the y direction. Hence the leading-order profile is given by (17) with the height $h_0(y)$ at the squeegee varying slowly along its length. We balance the flux into the bow wave from $x = \infty$ due to translation with the outward flux due to the lateral pressure gradient:

$$y = \int_0^{[h_0(y)^2 - 1]/2B} -\frac{1}{6}Z^2(3h - Z)\frac{\partial h}{\partial y}\, dx. \tag{19}$$

At this point, we need to eliminate the yield height Z and the derivation diverges from the Newtonian case. We substitute for $Z^2(3h - Z)$ from (16) (which holds provided variations in the x direction dominate those in the y direction) and use (17) to evaluate the derivatives. As a result, the flux balance (19) becomes

$$y = -h_0\frac{dh_0}{dy}\int_1^{h_0(y)} \frac{h(h - 1)}{B^2}\, dh. \tag{20}$$

Carrying out successive integrations furnishes

$$\frac{B^2}{2}(\mathcal{L}^2 - y^2) = \frac{h_0^5}{15} - \frac{h_0^4}{8} + \frac{h_0^2}{12} \tag{21}$$

and, to leading order for $B\mathcal{L} \gg 1$, we deduce that

$$h_0(y) \sim \left(\tfrac{15}{2}\right)^{1/5} B^{2/5}(\mathcal{L}^2 - y^2)^{1/5}, \quad X(h_0) \sim \tfrac{1}{2}\left(\tfrac{15}{2}\right)^{2/5} B^{-1/5}(\mathcal{L}^2 - y^2)^{2/5}. \tag{22}$$

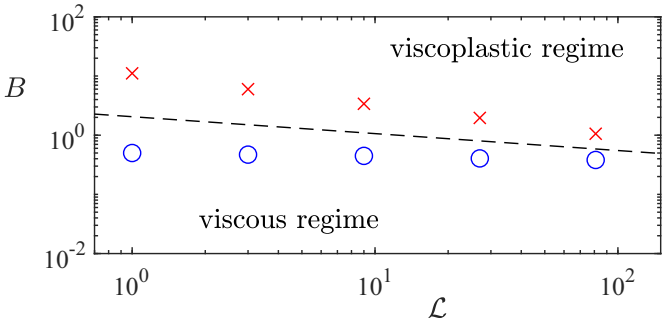

FIG. 6. $(\mathcal{L}, B)$-parameter space. The dashed line represents parameters for which the Newtonian and Bingham theories predict the same maximum thickness ($B \sim \mathcal{L}^{-2/7}$). The red crosses and blue circles represent where the maximum thickness from the numerical results has a 20% difference from the viscoplastic and Newtonian theory, respectively.

The flow thickness in the bow wave is given by (17) and (22 a), and $Z \approx [2(h-1)/B]^{1/2}$ as before. These predictions for the flow thickness and the yield height compare well to the numerical results along the center line and at the squeegee in Figs. 3(c) and 3(d), respectively. As in the Newtonian case, the asymptotic prediction breaks down near the ends of the squeegee.

To determine the condition that variations in the x direction dominate those in the y direction, we use (22) to estimate $\partial h/\partial x \sim B^{3/5}\mathcal{L}^{-2/5}$ and $\partial h/\partial y \sim B^{2/5}\mathcal{L}^{-3/5}$. Hence we require $\mathcal{L} \gg B^{-1}$, which is the same as the condition for $h_0 \gg 1$. Note that we have been assuming $B \gg 1$ so that $Z \ll h$ throughout the flow, so this condition is weaker than $\mathcal{L} \gg 1$.

In the bulk of the bow wave, we have $h \sim B^{2/5}\mathcal{L}^{2/5}$ and $Z \sim B^{-3/10}\mathcal{L}^{1/5}$. Hence $Z \ll h$ provided that $B \gg \mathcal{L}^{-2/7}$. If now $\mathcal{L} \gg 1$ and $1 \gg B \gg \mathcal{L}^{-2/7}$, then the above solution applies to the bulk of the bow wave, but there will be a region around its edge where the flow is almost completely yielded rather than almost completely plugged; if $\mathcal{L} \gg 1$ and $B \ll \mathcal{L}^{-2/7}$, then the flow is almost completely yielded everywhere and the Newtonian solution of Sec. II B applies. Figure 6 compares the numerical results to the dividing line between the Newtonian and Bingham theories.

Finally, we note that the quasiplugged shape given by (17) applies to any viscoplastic fluid with $B \gg 1$, since it arises simply from the condition of marginal yielding at the base. It follows that identical analysis and leading-order results, such as (22), apply for a Herschel–Bulkley fluid or, indeed, any inelastic viscoplastic fluid with a sufficiently large yield stress that $Z \ll h$. This can be seen by replacing $Z^2(3h - Z)$ in (16 a) and (19) with any function of Z and h; the expressions of (22) can then be reproduced. In contrast, the Newtonian analysis of Sec. II could be adapted for other constitutive laws without a yield stress, such as the power-law model, but the leading-order terms would then be different to the Newtonian case.

C. Snowplow problem

Consider the snowplow problem with the same geometry as Sec. II C and the Newtonian fluid replaced by Bingham fluid. The x' gradient of the flow thickness (perpendicular to the squeegee) dominates along most of the squeegee and the quasiplugged approximation ($Z \ll h$) corresponds to

$$h + \frac{B}{\partial h/\partial x'} = 0, \tag{23}$$

which furnishes the leading-order shape

$$h = [h_0(y)^2 - 2Bx']^{1/2}. \tag{24}$$

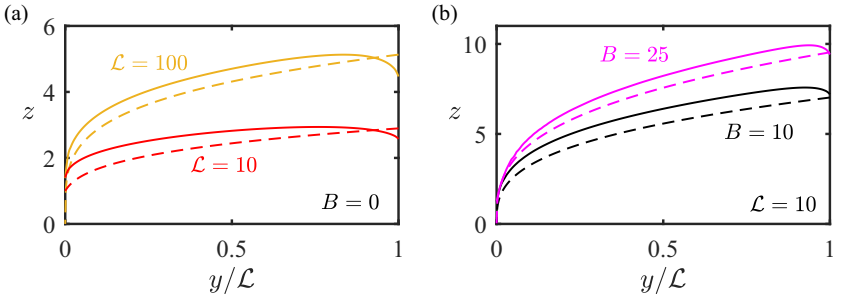

FIG. 7. Flow thickness at a squeegee ($x' = 0$) with angle $\alpha = \pi/3$. Comparison between the numerical results (continuous lines) and the theory (dashed lines) for (a) Newtonian fluid and (b) Bingham fluid.

The flux into the bow wave from upstream is balanced by the flux parallel to the squeegee, which is dominated by advection,

$$y = \sin\alpha \int_0^{(h_0^2-1)/(2B)} (h-1)\, dx'. \tag{25}$$

Substituting for h from (24), we find that the height of the bow wave at the squeegee satisfies

$$By = \sin\alpha \left[\frac{h_0^3}{3} - \frac{h_0^2}{2} + \frac{1}{6} \right]. \tag{26}$$

To leading order for $h_0 \gg 1$, the height of the bow wave is given (away from the ends) by

$$h_0(y) = \left(\frac{3By}{\sin\alpha} \right)^{1/3}. \tag{27}$$

Similar to the Newtonian case, Eq. (27) can be applied to a curved squeegee making a local angle $\alpha(y)$ with the y axis; for example, a constant height is predicted for a semicircular squeegee.

Equation (27) is compared to the numerical results for a squeegee at angle $\alpha = \pi/3$ and Bingham numbers $B = 10$ and $B = 25$ in Fig. 7 alongside a similar comparison for the Newtonian case.

The x' component of the governing equation, after integrating with respect to x' and using $Z \ll h$, is given by

$$(1-h)\cos\alpha - \frac{1}{2} Z^2 h \frac{\partial h}{\partial x'} = 0. \tag{28}$$

This can be rearranged to obtain an expression for the height of the yield surface,

$$Z = \left(\frac{2(h-1)\cos\alpha}{B} \right)^{1/2}. \tag{29}$$

We note that $h \sim \mathcal{L}^{1/3} B^{1/3}$ and $Z \sim \mathcal{L}^{1/6} B^{-1/3}$ so the condition $Z \ll h$ corresponds to $B \gg \mathcal{L}^{-1/4}$. As for the perpendicular squeegee, the limiting case $B \sim \mathcal{L}^{-1/4}$ matches to the results for a Newtonian fluid.

IV. CONCLUSION

In this paper, we have presented simple predictions for the flow thickness upstream of a squeegee that moves steadily through a layer of fluid. The theory shows good agreement with numerical integration of the governing lubrication model. The theoretical analysis is based upon approximating the flow as two dimensional since the squeegee is relatively long and then balancing the flux into the bow wave from translation with the lateral flux out owing either to hydrostatic pressure gradients or

to translation depending on the inclination of the squeegee. Separate analysis has been developed for Newtonian and viscoplastic fluids but the simple flux-balance ideas can be extended to other rheologies such as power-law or Herschel–Bulkley fluids, and to other settings such as flow in porous media and microfluidic applications where the dominant pressure gradients are associated with surface tension. In each case, the key is to determine the quasisteady cross section of the "bow wave" normal to the obstacle and then consider the flux associated with the slow variation along the obstacle.

ACKNOWLEDGMENTS

E.M.H. is grateful to the School of Mathematics and Statistics at the University of Melbourne for the award of a Harcourt–Doig research fellowship.

[1] H. R. Dietterich, K. V. Cashman, A. C. Rust, and E. Lev, Diverting lava flows in the lab, Nat. Geosci. **8**, 494 (2015).
[2] A. Ross, S. Wilson, and B. Duffy, Blade coating of a power-law fluid, Phys. Fluids **11**, 958 (1999).
[3] G. S. White, C. J. W. Breward, P. D. Howell, and R. J. S. Young, A model for the screen-printing of Newtonian fluids, J. Eng. Math. **54**, 49 (2006).
[4] M. Taroni, C. J. W. Breward, P. D. Howell, J. M. Oliver, and R. J. S. Young, The screen printing of a power-law fluid, J. Eng. Math. **73**, 93 (2012).
[5] E. M. Hinton, A. J. Hogg, and H. E. Huppert, Viscous free-surface flows past cylinders, Phys. Rev. Fluids **5**, 084101 (2020).
[6] A. Sauret, N. J. Balmforth, C. P. Caulfield, and J. N. McElwaine, Bulldozing of granular material, J. Fluid Mech. **748**, 143 (2014).
[7] H. K. Moffatt, Viscous and resistive eddies near a sharp corner, J. Fluid Mech. **18**, 1 (1964).
[8] B. W. Thompson, Secondary flow in a Hele-Shaw cell, J. Fluid Mech. **31**, 379 (1968).
[9] D. Davis, J. Suppe, and F. A. Dahlen, Mechanics of fold-and-thrust belts and accretionary wedges, J. Geophys. Res. B **88**, 1153 (1983).
[10] T. V. Ball, C. E. Penney, J. N. Neufeld, and A. C. Copley, Controls on the geometry and evolution of thin-skinned fold-thrust belts, and applications to the Makran accretionary prism and Indo–Burman ranges, Geophys. J. Int. **218**, 247 (2019).
[11] S. Puleo, *Dark Tide; The Great Molasses Flood of 1919* (Beacon Press, Boston, 2010).
[12] G. K. Batchelor, *An Introduction to Fluid Dynamics* (Cambridge University Press, Cambridge, UK, 1973).
[13] E. M. Hinton, A. J. Hogg, and H. E. Huppert, Shallow free-surface Stokes flow around a corner, Philos. Trans. R. Soc. A **378**, 20190515 (2020).
[14] N. J. Balmforth and R. V. Craster, A consistent thin-layer theory for Bingham plastics, J. Non-Newtonian Fluid Mech. **84**, 65 (1999).
[15] N. J. Balmforth, A. S. Burbidge, R. V. Craster, J. Salzig, and A. Shen, Visco-plastic models of isothermal lava domes, J. Fluid Mech. **403**, 37 (2000).